Chall. Nano Micro Scale Sci. Tech., 9(1): 12-22, Winter and Spring 2021
DOI: 10.22111/CNMST.2021.38805.1213

ORIGINAL RESEARCH PAPER

The Magnetic Field Application on Heat Transfer of Nanofluid Flow in a Flatten Tube: CFD Simulation

Somayeh Davoodabadi Farahani*, Mahdi Alibeigi, Hamed Hossienabadi Farahani

Department of Mechanical Engineering, Arak University of Technology, 38181-41167, Arak, Iran

Received 7 June 2021; revised 14 August 2021; accepted 14 August 2021 available online 2 September 2021

ABSTRACT: In this study, the efficacy of magnetic field on the two-phase nanofluid flow in the flattened tube was numerically examined. Initially, the finite volume method was used to solve the flow field and temperature. Secondly, the two-phase flow model was utilized to simulate the nanofluid flow. The consequences are associated with previously published data and good agreement observed. Thirdly, the uniform magnetic field is presumed to be constant, non-uniform, and oscillating. The results indicate that heat transfer and friction coefficient enhance with growing flatness and the nanofluid volume fraction. In the case of the constant magnetic field is exerted in the three directions, the Nusselt number increases by about 2.5%. The 90° phase delay in the oscillating magnetic field improves the heat transfer coefficient by 2%. The non-uniform magnetic field of 0.5 Tesla rather than without magnetic field in volume fraction of 0.01- 0.05 the heat transfer coefficient increases in about 1.6 – 2 times rather than the first mode. In addition, the velocity and temperature profile approached the uniform manner.

KEYWORDS: *heat transfer; non-uniform and oscillating magnetic field; Nanofluid; flattened tube*

INTRODUCTION

The cooling process with the help of fluids has important applications such as power generation, transportation, machining, and electronics. Currently, heat transfer equipment requires downsizing and increasing heat transfer intensity per unit area. Accordingly, the fluids have low thermal properties while metals have three times higher heat conduction coefficient than fluids, for instance, water and ethylene glycol. So, they have a restricted heat transfer capability, therefore in recent decades, the use of nanoparticles and fluid has been proposed to improve heat transfer. In recent years, in addition to the usage of fluid as a cooling fluid due to increasing heat transfer coefficient, researchers are interested in hydrodynamic and thermal control, which is one of the suitable methods, they applied the magnetic fluid field application for thermal controlling. Magnetic nanofluid or ferrofluid is a specific type of nanofluids that are highly stabilized magnetic nanoparticles with dimensions of about 3 to 15 nm in single-phase fluids consist of water or oil. It is possible to control the hydrodynamic and thermal behavior of this kind of fluid by applying the magnetic field in different directions and different directions, which is an essential advantage of this type of nanofluid usage[1]. Lately, due to research needs and commercial uses of mechanical devices, micro and nano dimensions are very common, the microchannel is used to transport fluid with different purposes such as heat transfer, movement, and fuel. Another microchannel application has led to the attention of researchers to microchannel using such as flow in the capillaries and other vital tissues with dimensions of micro, computer chips, etc.[2].

Rashidi et al.[3] investigated the nanoparticle's role in the productivity of passive solar distillation systems. They showed that numerical and mathematical modeling obtained some correlations that are very cooperative to satisfy the productivity coefficient and heat transfer in predicting the performance of these systems. They investigated the application of nanofluids in Distillation tower and evaporation systems. They indicated that the usage of nanofluid causes an intensification in heat transfer coefficients are one of the most essential factors of the passive solar distillation systems, which are used to transport fluid with different purposes such as convective heat transfer, and fuel. study of similar systems in microchannels such as flow in the capillaries and other vital human tissues with dimensions of micro, computer chipset, etc., has led to this field of attention to researchers. [4, 5]

AbdRabo et al.[6] numerically studied one type of flattening tube to find the best optimal and flatness range. Therefore, the device has been developed and examined experimentally.

Maki et al.[7] numerically, premeditated in two modes for the heat transfer of flattened tube consist of finned tube and non-finned tube. They observed that in the finned mode, the Nusselt number increases rather than the non-finned tube. When the micro finned shape changes from circle to square, the Nusselt number increases 8.5%. By changing the shape of the micro fin of the circle to a triangle, the Nusselt number increases 18.4%.

*Corresponding Author Email: *sdfarahani@arakut.ac.ir*
Tel.: +989183629703; Note. This manuscript was submitted on June 7, 2021; approved on August 14; published online September 2, 2021.

Nomenclature

A	fluctuation ranges	μ	viscosity (Pa.s)
Cp	specific heat capacity (J/kg/K)	μ_B	magnetic permeability (H/m)
D	diameter (m)	∇	gradient
f	fluctuation range	ϕ	volume friction
h	height (m)	φ	phase delay
I	electric current (A)	κ	diffusion coefficient
k	thermal conductivity ($\frac{W}{mK}$)	μ	density (kg/m^3)
m_p	magnetic moment	ρ	density (kg/m^3)
Nu	Nusselt Number		**subscript**
P	Pressure (Pa)	0	vacuum
Re	Reynolds Number	dr	drift
R	desired location	f	fluid
T	temperature (K)	in	input
V	velocity (m/s)	mi	mixture
w	width (m)	m	mean
	Greek Letters	p	particle
λ	Convection heat transfer coefficient $\left(\frac{W}{m^2K}\right)$	w	wall

Although, the friction coefficient in the non-finned tubes is lower than all types of micro-finned tubes and the micro-finned tube with shapes of the circle is lower than the other micro-finned tube.

Ibrahim et al.[8] numerically explored the friction coefficient and the heat transfer under a uniform magnetic field in a duct with porous blocks. They reported that intensification of the magnetic field intensity causes an increased friction coefficient and heat transfer, Zhai et al.[9] reported the heat transfer enhancement under the magnetic field for water-iron oxide nanofluid. In numerical research, Chu et al.[10] reported that the heat transfer coefficient upgraded about 30 % under a magnetic field with the intensity of 4 e + 6 rise in an elbow.

Sheikholeslami et al.[11] selected a new numerical method to simulate the influences of the magnetic force and the radiative transfer of nanofluids through a highly porous medium. They considered the different amounts of radiation, the magnetic force, and flotation, they showed the effects of nanoparticles on the transfer. the nanofluid is inspected by water-alumina nanofluid. Their results exposed that the Brownian motion affects the thermal conductivity and fluid viscosity as well as by strengthening the magnetic forces, heat transfer decreased and it could be increased by radiation. Atashafrooz et al.[12] deliberated the forced convection heat transfer of the magnetic field under a specified elbow with the reciprocal nanofluid action, which has compared with the flow irreversibility with sudden contraction on the flow path. Their consequences demonstrated that the magnetic field application angle and Hartman number were the reason for the momentous intensification in the flow, while the inverse efficacy has an adverse effect on the heat transfer rate. Also, the total entropy and average density increase with the nanoparticles volume fraction growing. Sajjadi et al.[13] simulated a three-dimensional magneto-hydrodynamic natural convection heat transfer in a cubic chamber with a one-way sinusoidal temperature distribution. One of the conclusions of this study is that rising the Hartmann number reduces the heat transfer rate while increasing the Rayleigh number and the volume fraction of nanoparticles will increase the heat transfer rate. In another study, Sajjadi et al.[14] investigated the natural convection heat transfer of Magnetohydrodynamics (MHD) in a cubical hole with the application of a numeric method. They pointed out that the Hartman number effectiveness on the heat transfer rate increases with the growth of the Grashof number, as the Nusselt number is observed between 12 - 71 % with an increase of Hartmann number from 0 to 100.

According to previous studies, few studies have been done to explore the magnetic field efficacy types on heat transfer on the channel. In this study, the effect of several magnetic field application types on the nanofluid heat transfer from a flattened tube, where include the uniform, oscillating and non – uniform has been inspected. Nanofluids are considered a two-phase flow. The finite volume method is employed to solve the flow and temperature field. The influence of volume fraction and

change of nanofluid on heat transfer have been investigated.

NUMERICAL MODELING

In this case, the forced convection heat transfer inside a flattened tube with the magnetic field action has been investigated. A schematic of the desired geometry is visualized in Fig. 1a.

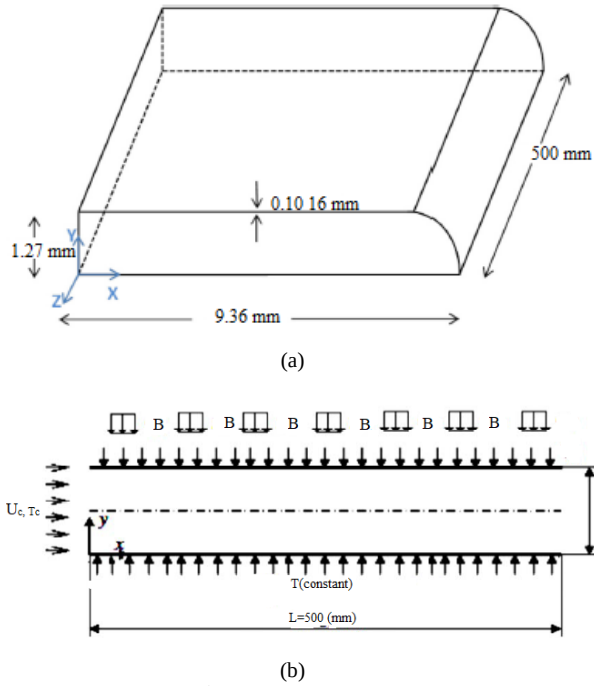


Fig. 1. a) a diagram of the case study and **b)** boundary condition

Considering the incompressible fluid and the steady flow, the momentum equations of momentum and energy are defined as follows [15];

$$\nabla.(\rho V) = 0 \quad (1)$$

$$\rho V.\nabla T = -\nabla P + \nabla.(\mu.\nabla V) \quad (2)$$

$$\rho V.\nabla T = \nabla.(k\,\nabla T) \quad (3)$$

Where, ρ, μ, k, P, and T are the density, dynamic viscosity, thermal conductivity coefficient, pressure, velocity, and fluid temperature, respectively. When Nanofluid is operated as a working fluid, the mixture model is used to solve. Two phases of fluid or particle are modeled by solving the equations of continuity, momentum, energy, and volume fraction of the second phase, considering the relative velocity of zero or non – zero velocities between two phases. In this model, it is assumed that the phases in the continuous field and each phase have a velocity vector associated with itself, and within each control volume. There is a volume fraction of the initial phase and a volume fraction of the secondary phase. The equations of continuity, momentum, energy, and volume fraction are expressed as follows.[16]

The continuity equation can be assumed as;

$$\nabla.(\rho_{mi}.V_{mi}) = 0 \quad (4)$$

The momentum equation calculated in this relation;

$$\nabla.(\rho_{mi} v_{mi}.\overrightarrow{V_{mi}}) = -\nabla P + \nabla.(\mu_{mi}\nabla\overrightarrow{V_{mi}}) + \nabla.(\phi\rho_p v_{dr,p}\nabla\overrightarrow{V_{dr,p}}) \quad (5)$$

Energy equation is determined as;

$$\nabla.\left[(\phi\rho_p Cp_p\overrightarrow{V_p} + (1-\phi)\rho_f Cp_f\overrightarrow{V_f})T\right] = \nabla.(k_{mi}\nabla T) \quad (6)$$

The volume fraction equation considered as,

$$\nabla.(\rho_{mi} v_{mi}) = -\nabla.(\phi\rho_p v_{dr,p}) \quad (7)$$

Where, $\overrightarrow{V_{dr,p}}$ and $\overrightarrow{V_{mi}}$ are the drift velocity and mean mass velocity which calculated from the following relationships: [16]

$$\rho_{mi}\overrightarrow{V_{mi}} = \phi\rho_p\overrightarrow{V_p} + (1-\phi)\rho_f\overrightarrow{V_f} \quad (8)$$

$$\overrightarrow{V_{dr,p}} = \overrightarrow{V_{pf}} \quad (9)$$

$$\overrightarrow{V_{pf}} = \overrightarrow{V_p} - \overrightarrow{V_f}$$

In the attendance of the magnetic field, the momentum equation and the energy equation are expressed as follows[17]:

$$\rho(\vec{V}.\nabla\vec{V}) = -\vec{\nabla}P + \mu\nabla^2\vec{V} + \mu_0(\vec{M}.\nabla)\vec{B} + \vec{J}\times\vec{B} \quad (10)$$

$$\rho C\vec{V}.\nabla T = k\nabla^2 T + \frac{\vec{J}\times\vec{B}}{\sigma_m} \quad (11)$$

Where, μ_0 , $\vec{M}$, σ_m , and $\vec{B}$ are the Magnetic permeability in the vacuum, Magnetic susceptibility, electrical conductivity, and magnetic field intensity, respectively. It is also $\vec{J}$ is the electric current intensity which can be calculated from the following equation,

$$\vec{J} = \frac{\nabla\times B}{\mu_B} \quad (12)$$

Where, μ_B is the magnetic permeability. M is calculated from the following equation:[17]

(13)

$$M = \frac{6m_p}{\pi d_p^3}\left\{\coth\left(\frac{\mu_0 m_p B}{K_b T}\right) - \frac{K_b T}{\mu_0 m_p B}\right\}$$

Where, m_p, d_p, and K_b represent a magnetic moment, magnetic particle diameter, and Boltzmann constant, respectively. The magnetic field due to electric current (or electrical voltage)is defined as follows [17]:

$$\vec{B} = \frac{I}{2\pi\left((x-a)^2 + (y-b)^2\right)}\left(-(y-b),(x-a)\right) \quad (14)$$

Where, I and (a, b) are the location of the electric current and the amount of electric current. In this study, electrical voltage is used which can be calculated using Ohm's law of electric current intensity. The oscillating magnetic field is defined as [16];

$$\vec{B} = B_0\left(1 + A\cos\left(2\pi ft - \kappa R + \varphi\right)\right) \quad (15)$$

Where, B_0, A, f, κ, R, and φ are respectively the mean value of the magnetic field, fluctuation range, frequency, diffusion coefficient, desired location, and phase delay.

The Reynolds number (Re) is defined as follows,

$$\mathrm{Re} = \frac{\rho_f V_{in} D}{\mu_f} \quad (16)$$

Where V_{in}, and D represent the inlet velocity and diameter of the flattened tube. The Nusselt number and, the convective heat transfer coefficient is calculated as follows:

$$Nu = \frac{\lambda D}{k_f} \quad (17)$$

$$\lambda = \frac{-k_f \left.\frac{\partial T}{\partial y}\right|_{channel/swall}}{T_w - T_m} \quad (18)$$

Where, T_w is the wall temperature and T_m is the average fluid temperature within the channel. The boundary conditions are shown in Fig.1b. The no-slip condition was used on the solid wall and the wall temperature is constant and equal to T_w. The velocity and the fluid temperature into the tube are uniform and equal to T_C and U_C, respectively.

The outflow boundary condition is considered at the channel output. The magnetic field (B) is exerted on the tube's wall. The thermophysical properties of fluids are assumed to be constant. The base fluid is water and the nanoparticle diameter of 0.1 nanometers. The material properties used in the calculations are exposed in Table 1.

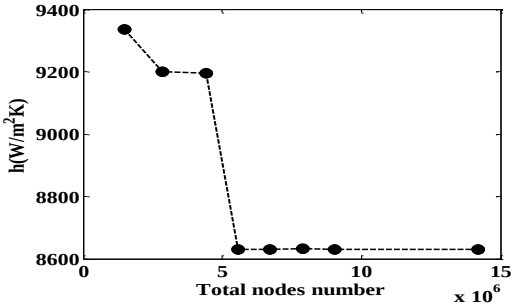
Table 1
Properties of material and passing fluid[9]

Property	Steel	CuO	Fe3O4	AL2O3	Water
Cp [J.kg^{-1}K^{-1}]	0.87	540	670	765	4182
ρ [kg.m^{-3}]	2719	6500	5200	3600	998
k[W.m^{-1}.K^{-1}]	202.4	18	6	36	0.6
μ [Pa.s]	-	-	-	-	0.000855

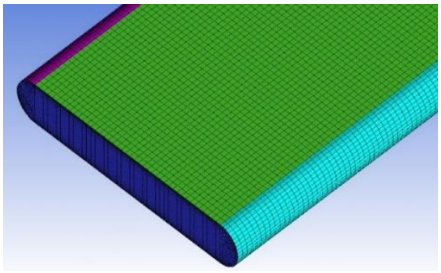
GRID INDEPENDENCY AND VALIDATION

In most numerical flow field research, the finite volume method is employed to discretize the momentum and energy equations, which are done second-order upwind and the pressure discretization takes place in a standard form. The coupling of pressure and velocity is also carried out in the SIMPLE algorithm. The Under-Relaxation Factor of pressure is 0.3 and the Under-Relaxation Factor of density, volume, and energy equal 1, and the Under-Relaxation Factor of the momentum was considered equal to 0.7. To investigate the grid independence of the numerical solution, in return for boundary conditions and certain geometrical variables, the simulation has been done and the same process is repeated several mesh sizes. The k-ω SST turbulence model is used for the state where the flow is turbulent. This model simultaneously has the competence of the k-ω model in areas with low Reynolds and the high quality of the k-ε model in areas with high Reynolds. To find a suitable grid that results are in the grid independence from the meshes, there is a forced conversion coefficient for a flatten tube containing a water fluid for the meshes with different points obtained in Fig. 2 a. In meshing the solution domain, the mesh has been tried to be small enough near the wall.

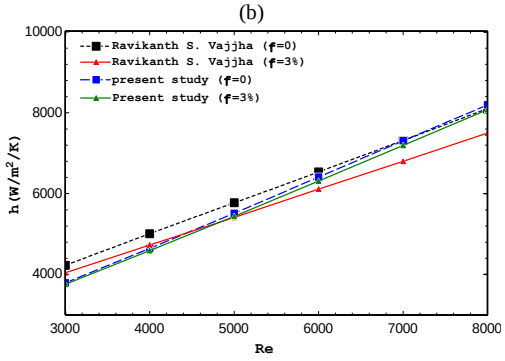
According to the obtained results, the grid with an 8million node is chosen to continue studies. The selected mesh is shown in Fig. 2b., To authorize the numerical modeling presented in the present study, the results of reference Vajjha et al.[18] have been validated and the results of this comparison for the water and water-nanoparticle 3% shown in Fig. 2C. The results have a difference meanly about 7 % with results Vajjha et al.[18]. There is also a good agreement with the results of reference Vajjha et al.[18] in this method.



(a)



(b)

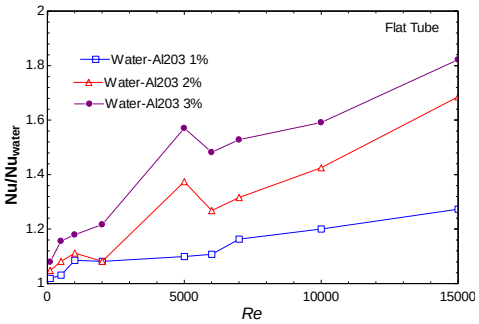


(c)

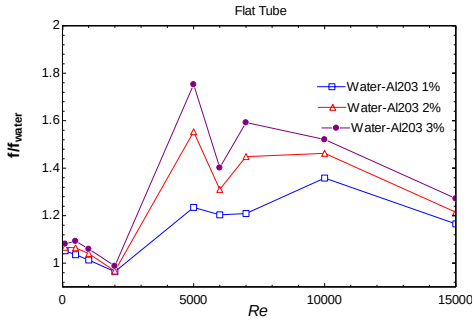
Fig.2. a) Check grid independency and **b)** Selective mesh in this study and **c)** validation of the present study

RESULT AND DISCUSSION

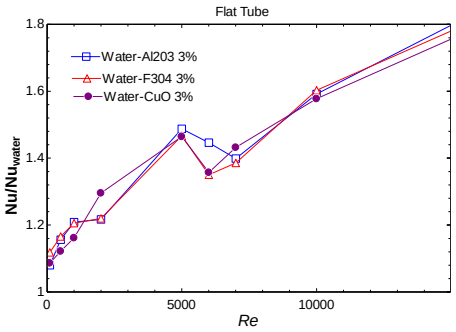
In this section, the efficacy of various magnetic fields on heat transfer inside the flattened tube is inspected. The effect of exerting water-Al2O3 nanofluid on Nusselt number and friction coefficient for Reynolds numbers and different volume fractions is investigated and presented in Fig.3. In the laminar and turbulent flow, adding nanoparticles to the working fluid increases the thermal conductivity and viscosity of the nanofluid. Enlarging of nanoparticle volume fraction is the cause of the Nusselt number and friction coefficient expansion. The percentage of the Nusselt number alteration for volume fraction of 1%, 2% and 3% was averagely 5%, 5% and 11%, respectively, also for friction coefficient is about 3%, 6% and 8 %, respectively. The mechanism of heat transfer in nanoparticles can also be comprehensible with the associates of quantum physics theories. It is assumed that heat transfer in nanoparticles is done by phonons.



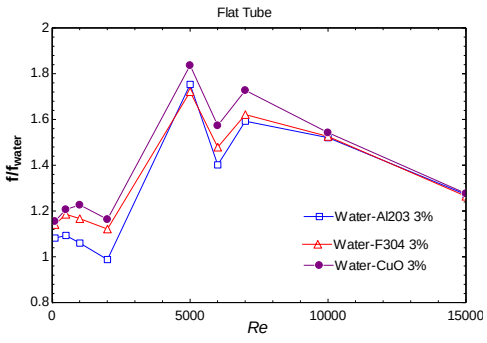
(a)



(b)



(c)



(d)

Fig. 3. a) heat transfer and **b)** friction coefficient for the different volume fractions on, the effect of different nanoparticles on **c)** heat transfer and **d)** friction coefficient.

Mean Free Path (MFP)in the particle collection is known as the distance that a particle must move to deal

with the other between successive impacts. To make this happen, the MFP of Phonons is smaller than the diameters of particles, while the particles are smaller than those of these Phonons, and the motion within nanoparticles is similar to that of one side of the nanoparticles. In the opinion of the researchers, the impacts of these Phonons in nanoparticles are the cause of the heat transfer phenomenon. Accordingly, the presence of nanoparticles action is the fluid temperature extension; correspondingly, the heat transfer rate develops due to increasing the fluid viscosity, the similarity coefficient, and friction coefficient, the coefficient of friction is increased. The effect of copper nanoparticles, Fe3O4, and copper oxide on heat transfer and friction factor. A schematic of the tube flattening rate is shown in Fig. 4a. The effect of the flattening rate on the Nusselt number in the three-volume fraction of the nanofluid is shown in Figs.4b&c. As the increase in the flattening rate increases the Nusselt number and the friction coefficient increase. The increase of heat transfer in the vertical direction (high and low wall) decreases with average fluid temperature $(T_w - T_m)$ which is due to increasing heat transfer coefficient in the flat tube. It is possible to say that in flatten tubes; the thermal resistance of fluid is lower than that of fluid heat in the tube. The Nusselt number, and the friction coefficient increase as the growing of flatness rate, the maximum velocity, and velocity gradient increase in the tube. As the cross-section area gets out of the regular mode, the shear stress at the corners is reduced to the wall. The influx of the constant magnetic field is shown for Re=500 and 10000 for different nanoparticles and the different volume fractions of heat transfer and friction coefficient in Figs.5&6. The rate of change in heat transfer at Re = 500 for Al2O3, Fe3O4, and CuO nanoparticles compared to the single-phase state is 1%, 1%, and 2%, respectively. At Re = 10^4, it is 2%, 3% and 3, respectively. For friction coefficient in Re = 500 compared to single-phase mode, 2%, 2% and 3%, respectively, and in Re = 10^4, it is equal to 1%, 3% and 2%, respectively. The cause of this behavior is the magnetic field impression on the flow pattern.

This effect causes the formation of three kernel zones, the Hartman layer, and lateral layers on the channel.

The presence of the magnetic field around the channel causes the formation of the Hartman layer near the channel wall. The shear stress near the wall is very strong so that adhesion forces can compete with the magnetic forces in the Hartman layer alongside the channel wall. By applying the magnetic field, two Kelvin and Lorentz force works as a positive term in the momentum equation and the term joule term is added to the energy equation.

In the case where the magnetic field is constant, the magnetic field gradient is zero in the flow field, and the Lorentz force is applied to the walls of the channel, which has a significant effect on the heat transfer rate and friction coefficient.

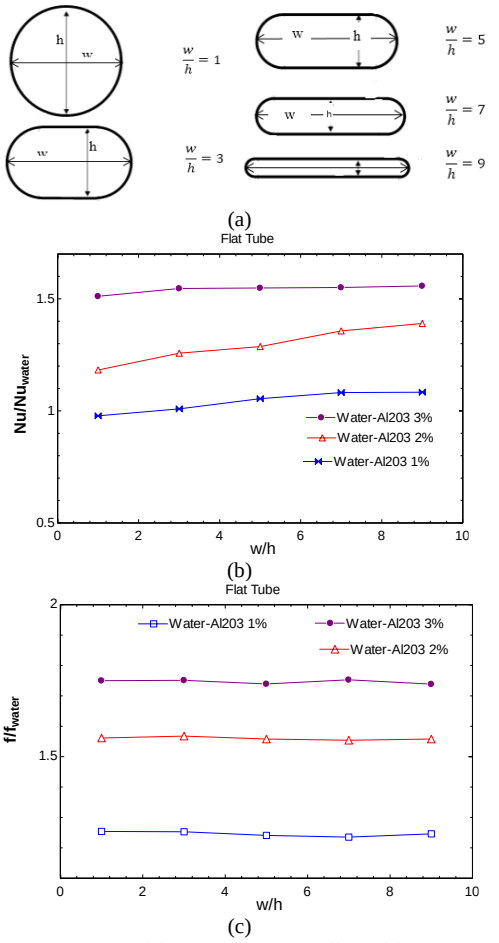


Fig. 4. a) schematic of flattening rate, the effect of flatness rate on **b)** Nu/Nu $_{water}$ and **c)** f/f$_{water}$

The suspension of nanoparticles in fluid leads to increasing the thermal conductivity coefficient of the nanofluid. This action expands when the liquid and nanoparticle composition is placed under a magnetic field. Some mechanisms, such as particle transmission, viscosity gradient, Brownie motion, and disturbance in the thermal boundary layer are the reason for heat transfer enhancement. The external magnetic field causes the magnetic particles to be attracted to the sidewall and the particle transfer procedure increases. Increasing the strength of the magnetic field causes an increase in heat transfer. Besides, the increase in volume percentages in the presence of the magnetic field will increase the heat transfer. In the present study, the magnetic field has been applied in three directions. The influx of the magnetic field of 10 Tesla in the three main directions, and separately for the water-iron oxide fluid, is shown in Fig.7.

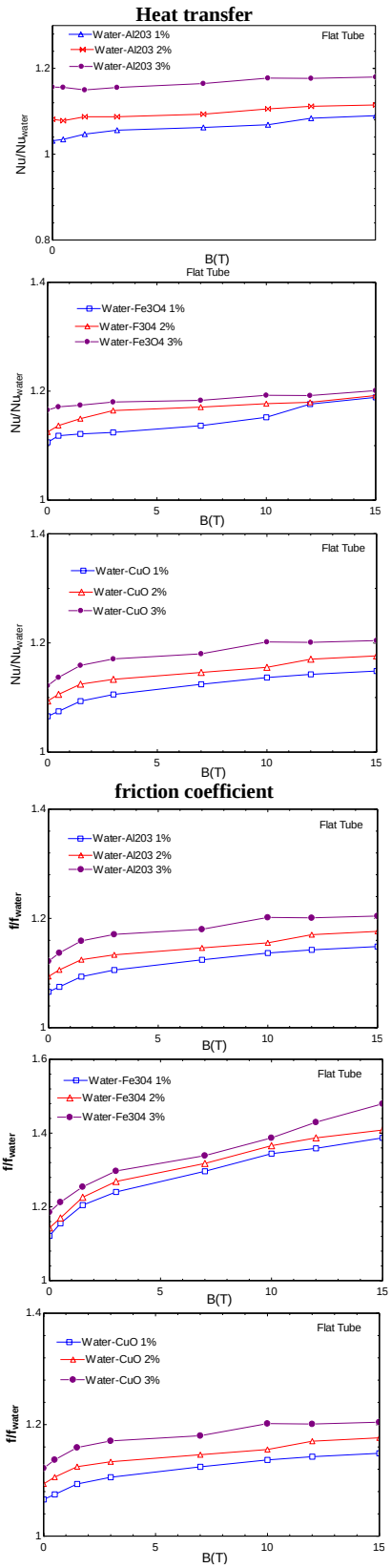


Fig. 5. A consequence of constant magnetic field on heat transfer and friction coefficient in Re = 500

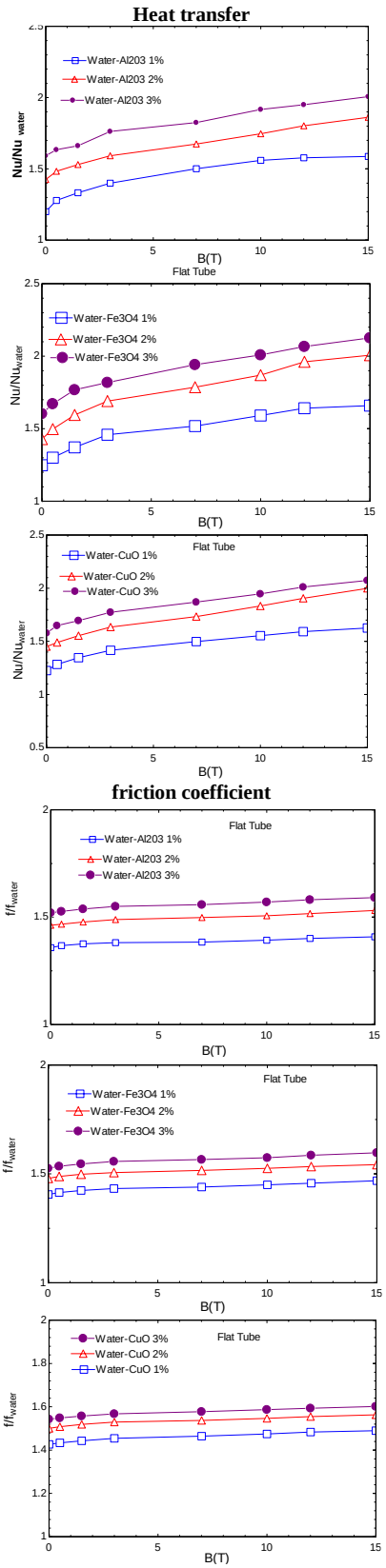


Fig. 6. A consequence of constant magnetic field on heat transfer and friction coefficient in Re = 10000

The results show that the changing of the Nusselt number in all three modes is almost identical. It is detected that in the case of applying the magnetic field in the three directions and at the same time, the Nusselt number increases by about 2.5 %. The reason for this is that, more magnetic particles are increased by exerting the magnetic field in the three directions. Correspondingly the heat transfer increases.

The usefulness of the oscillating magnetic field with phase delay on the heat transfer coefficient is shown in Fig.7d. By applying the phase delay in the direction of Y, to apply angle before applying angle 90 degrees in the direction of Y, there is no noticeable modification in the Nusselt number and the wall, but at an angle of 90 °, the magnetic particles are absorbed into the wall and the temperature gradient in the area increased and the Nusselt number improved. Another reason for this thermal treatment, in this case, is that the magnetic gradient field is calculated employing Maxwell's equations.

Moreover, the Lorentz force, the Kelvin force is applied to the flow field. The presence of Kelvin force causes vortex formation near the canal wall, which leads harmoniously in the magnetic field gradient. This gradient field is boosted accordingly with this magnetic field gradient. To explore the efficacy of non -uniform magnetic field on the wall of the electric voltage channel. Velocity and temperature contours at the non-uniform magnetic field B = 0.5 T & Fe3 O2-water at Re = 5000 The efficacy of exerting the non - uniform magnetic field on heat transfer in Re=5000 is investigated and shown in Fig.8a.

As the magnetic field intensifies, the heat transfer improves from 0 to 0.5 Tesla and then decreases and remains constant as the intensity of the magnetic field increases. The convective heat transfer coefficient is maximum at B= 5 Tesla for the reason that the power of the axial non-uniform magnetic field, the Lorentz force, and the Kelvin force increase. So, the vortex closes near the wall and causes an increase in the velocity gradient near the wall. according to the Chilton-Colburn analogy, the temperature gradient and finally the heat transfer rate increase.

Fig.8b shows that as the nanoparticle fraction increases, the effect of the non-uniform magnetic field increases. So that by increasing the volume fraction from 1 to 5%, the ratio of Nusselt number to field-less state is about 1.6-2 times. The change of velocity and temperature along the x-axis is shown in Figs.8c &d.

Due to the efficacy of the magnetic field, substantial changes in velocity and temperature profile are observed. Increasing the velocity profile, the more uniform velocity and the temperature gradient are increased near the wall.

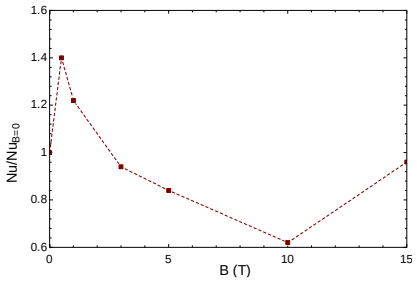
At low-velocity profiles, the velocity profile is M-shaped as the cause of this behavior is the presence of the Kelvin and Lorentz forces with the usage of the magnetic field. The contours of the velocity and temperature by applying the non - uniform magnetic field of B = 0.5 T in the two-phase model for the iron oxide particles in Re = 5000 in volume fraction are illustrated in Fig.9.

CONCLUSION

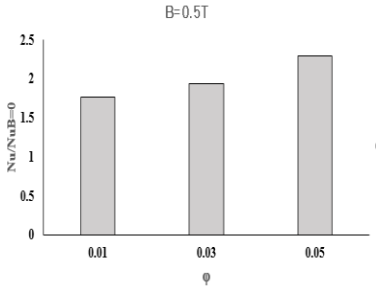
In this paper, the efficacy of the presence/lack of magnetic field on the heat transfer and flow of a nanofluid within a flattened tube is numerically inspected. To model the flow of nanofluids, a two-phase mixture model has been applied.

Originally, the magnetic field is supposed to be constant, nonuniform, and oscillating. The findings of the research are paraphrased as follows

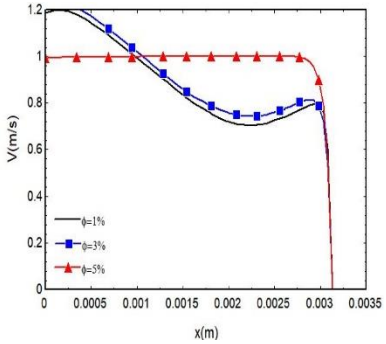
- The presence of nanoparticles in the fluid and increase in its volume fraction causes the average temperature of the fluid and shear stress to increase and leads to increased heat transfer and friction coefficient. The percentage variation of Nusselt number and friction coefficient with varying nanoparticle types is negligible.
- Due to the increase of flattening rate, the friction coefficients and the Nusselt number in flatten tubes increases to the circular tube.
- Between three magnetic fields: constant, oscillating, and non-uniform, the non-uniform magnetic field is more effective in improving heat transfer. In the non - uniform magnetic field with an increasing field intensity of 0.5 Tesla, there has been little effect on heat transfer. Eventually, the maximum heat transfer enhancement occurred at an intensity of 0.5 Tesla.



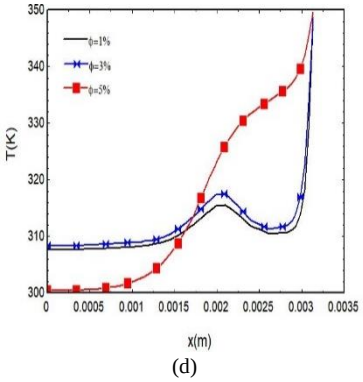
(a)



(b)

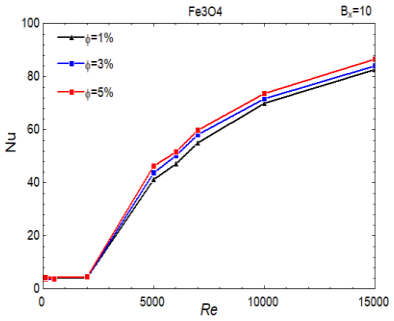


(c)

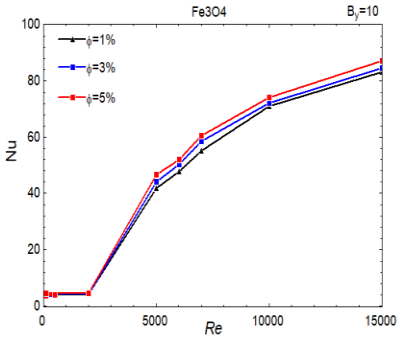


(d)

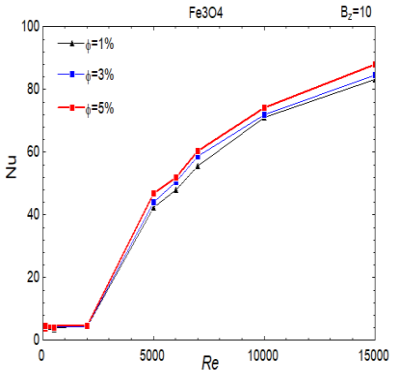
Fig. 8. a) variations in Nusselt number ratio and **b)** heat transfer coefficient of iron oxide nanoparticles in terms of the magnetic field, **c)** Velocity and **d)** temperature distribution at non-uniform magnetic field B = 0.5 Tesla on Fe_3O_2-water at Re = 5000



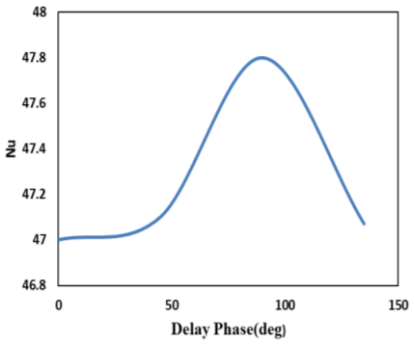
(a)



(b)



(c)



(d)

Fig. 7. Variations in Nusselt number according to Reynolds number in three-volume fractions of iron oxide nanofluids by exerting a magnetic field in three directions **a)** X and **b)** Y, **c)** Z and **d)** Nusselt number changes with phase delay in Y-axis with the oscillating magnetic field

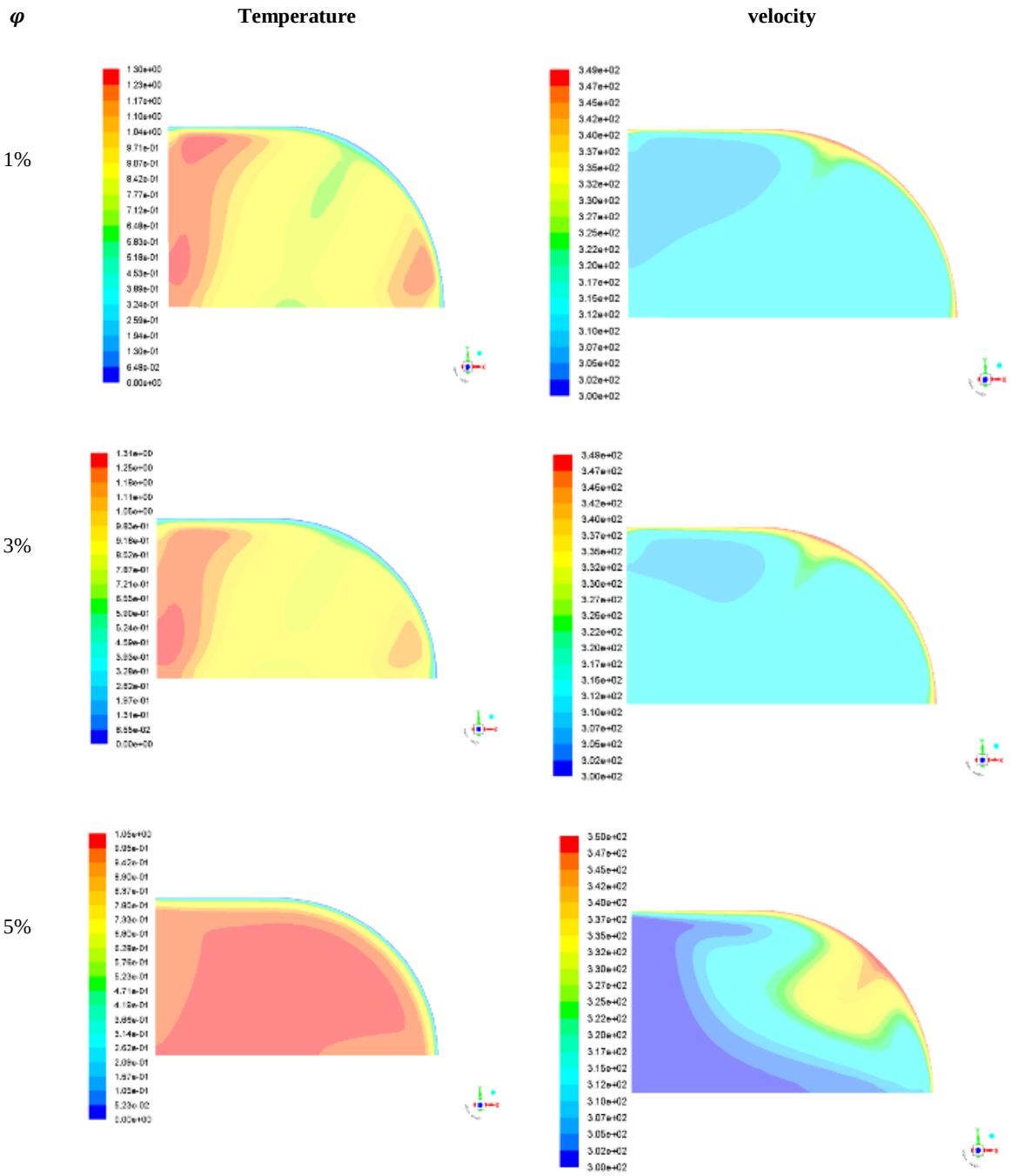


Fig. 9. Velocity and temperature contours at the non-uniform magnetic field B = 0.5 T & $Fe_3O_2 - water$ at Re = 5000

REFERENCES

[1] Choi S, Zhang ZG, Yu W, Lockwood F, Grulke E. Anomalous thermal conductivity enhancement in nanotube suspensions, Applied physics letters, 79(14) (2001) 2252-2254.

[2] Alibeigi M, Farahani S. Effect of Porous Medium Positioning on Heat Transfer of Micro-channel with Jet, International Journal of Engineering, 33(10) (2020) 2057-2064.

[3] Rashidi S, Karimi N, Mahian O, Esfahani JA. A concise review on the role of nanoparticles upon the productivity of solar desalination systems, Journal of Thermal Analysis and Calorimetry, 135(2) (2019) 1145-1159.

[4] Rashidi S, Mahian O,Languri EM. Applications of nanofluids in condensing and evaporating systems, Journal of Thermal Analysis and Calorimetry, 131(3) (2018) 2027-2039.

[5] Rashidi S, Eskandarian M, Mahian O, Poncet S. Combination of nanofluid and inserts for heat transfer enhancement, Journal of Thermal Analysis and Calorimetry, 135(1) (2019) 437-460.

[6] AbdRabo MF, Pasha KM. Controlling the heat transfer and pressure drop within economical working conditions for a movable flat tube bundle, International Journal of Thermal Sciences, 107 (2016) 259-271.

[7] Zaidan MH, Alkumait AA, Ibrahim TK. Assessment of heat transfer and fluid flow characteristics within finned flat tube, Case studies in thermal engineering, 12 (2018) 557-562.

[8] Ibrahim M, Saeed T, Bani FR, Sedeh SN, Chu YM, Toghraie D. Two-phase analysis of heat transfer and entropy generation of water-based magnetite nanofluid flow in a circular microtube with twisted porous blocks under a uniform magnetic field, Powder Technology, 384 (2021) 522-541.

[9] Zhai X, Qi C, Yang Y, Wang J. Thermo-hydraulic performance of nanofluids under adjustable magnetic field, Applied Thermal Engineering, 186 (2021) 116491.

[10] Chu YM, Moradi R, Abazari AM. Computational investigation of non-uniform magnetic field on thermal characteristic of nanofluid stream inside 1 8 0∘ elbow pipe, Modern Physics Letters B, 35(09) (2021) 2150157.

[11] Sheikholeslami M, Sajjadi H, Amiri Delouei A, Atashafrooz M, Li Z. Magnetic force and radiation influences on nanofluid transportation through a permeable media considering Al2O3 nanoparticles, Journal of Thermal Analysis and Calorimetry, 136(6) (2019) 2477-2485.

[12] Atashafrooz M, Sheikholeslami M, Sajjadi H. A. Amiri Delouei, Interaction effects of an inclined magnetic field and nanofluid on forced convection heat transfer and flow irreversibility in a duct with an abrupt contraction, Journal of Magnetism and Magnetic Materials, 478 (2019) 216-226.

[13] Sajjadi H, Delouei AA, Atashafrooz M, Sheikholeslami M. Double MRT Lattice Boltzmann simulation of 3-D MHD natural convection in a cubic cavity with sinusoidal temperature distribution utilizing nanofluid, International Journal of Heat and Mass Transfer, 126 (2018) 489-503.

[14] Sajjadi H, Amiri Delouei A, Sheikholeslami M, Atashafrooz M, Succi S. Simulation of three dimensional MHD natural convection using double MRT Lattice Boltzmann method, Physica A: Statistical Mechanics and its Applications, 515 (2019) 474-496.

[15] Dehghan M, Valipour MS, Saedodin S. Temperature-dependent conductivity in forced convection of heat exchangers filled with porous media: a perturbation solution, Energy Conversion and Management, 91 (2015) 259-266.

[16] Manninen M, Taivassalo V, Kallio S. On the ı model for multiphase flow, (1996).

[17] Hariri S, Mokhtari M, Gerdroodbary MB, Fallah K. Numerical investigation of the heat transfer of a ferrofluid inside a tube in the presence of a non-uniform magnetic field, The European Physical Journal Plus, 132(2) (2017) 1-14.

[18] Vajjha RS, Das DK, Namburu PK. Numerical study of fluid dynamic and heat transfer performance of Al2O3 and CuO nanofluids in the flat tubes of a radiator, International Journal of Heat and fluid flow, 31(4) (2010) 613-621.